

Probing the anomalous positron fraction origin with fully leptonic decaying gravitino dark matter candidates

Johannes Buchner,^{a,b} Edson Carquin,^e Marco A. Díaz,^c
Germán A. Gómez-Vargas,^{1a} Boris Panes,^{a,b,d} Nicolás Viaux^e

^aInstituto de Astrofísica, Pontificia Universidad Católica de Chile, Avenida Vicuña Mackenna 4860, Santiago, Chile

^bMillenium Institute of Astrophysics, Vicuña MacKenna 4860, 7820436 Macul, Santiago, Chile

^cInstituto de Física, Pontificia Universidad Católica de Chile, Avenida Vicuña Mackenna 4860, Santiago, Chile

^dInstituto de Física, Universidade de São Paulo, R. do Matão 187, São Paulo, SP, 05508-900, Brazil

^eDepartamento de Física y CCTVal, Universidad Técnica Federico Santa María, Casilla 110-V, Valparaíso, Chile

E-mail: johannes.buchner.acad@gmx.com, edson.carquin@fis.puc.cl,
mad@susy.fis.puc.cl, ggomezv@uc.cl, bapanes@if.usp.br, nviaux@fis.puc.cl

Abstract. The flux of positrons measured by the space-based experiments PAMELA, AMS-02, CALET, DAMPE and Fermi-LAT² shows an unexpected behaviour at high energies, in comparison with expectations from standard astrophysical sources. In particular, AMS-02 observations provide compelling evidence for a new source of positrons and electrons whose origin is still unknown. Satisfactory scenarios include either the contribution of dark matter or unresolved astrophysical sources, such as nearby pulsars. It has been shown that explanations based mostly on dark matter, tend to overproduce gamma-rays, entering in conflict with measurements of the extra-galactic gamma-ray background (EGB). Although this situation seems to be quite generic, it ultimately depends on the properties of the dark matter candidate. In this work we revisit a model in which the gravitino is a dark matter candidate decaying to SM particles through trilinear R-parity violating couplings. Compared to the bilinear scenario, our model produces more electrons and positrons and fewer photons. When considering AMS-02 data alone, this model is compatible with EGB constraints. However, when DAMPE or CALET measurements of the sum of electrons and positrons fluxes are considered without the AMS-02 data, tensions appear. Therefore, in order to evaluate this model further, discrepancies between the data collected by these experiments need to be clarified³.

Keywords: dark matter experiments, cosmic ray experiments, gamma ray experiments, dark matter theory

¹Now Corporate Data Scientist at [Dercó](#),

²I think this is not something measured y Fermi-LAT?

³I think we need to elaborate more about which conclusions could be extracted from this work

1 Introduction

The continuous and systematic analysis of the data collected by cosmic-ray space based detectors is one of the most direct ways¹ to check and test the predictions of particle physics models that contain a candidate for dark matter (DM) which can annihilate or decay to Standard Model (SM) particles. For a review focused on the gravitino dark matter scenario we refer to [1] and [2] for an updated and more general discussion.

Furthermore, this discussion becomes specially relevant since contemporary experiments present persistent and striking anomalies in cosmic-ray measurements. For instance, the energy spectrum of electrons and positrons measured by experiments such as PAMELA [3], AMS-02 [4–6], CALET [7], DAMPE [8] and Fermi-LAT [9] show noticeable discrepancies when compared to predictions based on standard astrophysical sources, such as cosmic-ray interactions or emissions from pulsars. Therefore, these experimental signals strongly suggest that extra sources of (primary) positrons are required in order to make sense of the data.

In particular, it has been shown that the positron anomaly, reported by experiments such as PAMELA [3] and AMS-02 [4], can be well explained by considering a population of DM in agreement with standard density profiles, such as NFW, that can annihilate or decay to charged leptons both as primary or secondary particles. This picture, however, seems to be in conflict with the measurements of the extra galactic gamma-ray background (EGB) derived from Fermi-LAT and other gamma-ray detectors [10–15]. Some of these explanations include modifications of (standard) DM density distributions. In general, it may be argued that a more realistic explanation of the anomalous data must include DM particles, probably with more “ad-hoc” properties in comparison with popular models, in addition to proper modelling of astrophysical sources [16][17]².

In order to contribute to this discussion, in a previous work [18] we tested a DM scenario that contain a gravitino as the lightest super-symmetric particle (LSP) and bilinear R-parity violation (BRpV) couplings. We found that this model is indeed able to explain the anomalous positron fraction measured by AMS-02 but at the cost of producing so many photons that get in serious conflicts with EGB limits. Furthermore, the parameter space that is preferred by AMS-02 data falls short to explain the observed scale of neutrino mass differences or their mixing angles, which was one of the main motivations to introduce BRpV to start with.

In the current work we propose a possible way to alleviate the tensions between gravitino DM scenarios and the current data. This is achieved by moving from bilinear to trilinear RpV couplings. Within the trilinear RpV coupling scenario, we can consistently model the data from AMS-02 and respect the EGB limits derived from Fermi-LAT data, which can be explained by the leptonic nature of gravitino decays in this model. However, when we include the data from CALET or DAMPE, that cover higher energies than AMS-02, the things get tougher again. Nonetheless, with our model we can link the life-time and branching fractions of gravitino decays fitting well the positron anomaly to the scale of neutrino physics. Ultimately, we acknowledge that this model probably should be complemented in order to properly account for both, cosmic-ray observations and neutrino physics.

The paper is organized as follows. In section 2 we describe the decaying gravitino DM model with trilinear RpV couplings. In section 3 and section 4 we present the results and predictions of our statistical analysis. In section 5 and appendix B we compare trilinear and

¹I suggest we rewrite this sentence since this is formally an indirect way to do it!

²**ADDED:** Refs from HAWC experiment and Hooper explanations

bilinear scenarios and show why the first could ameliorate the prospects for the gravitino DM hypothesis.

2 Gravitino model and effective decay channels

We consider a super-symmetric (SUSY) extension of the SM with a low energy spectrum characterized by a gravitino as the lightest SUSY particle (LSP), which can decay to trilepton, triquark or mixed triple particle final states by mean of trilinear R-parity violating couplings. We suggest to follow [1, 19] for details on the underlying theoretical model.

In this scenario, the decay of the gravitino LSP can be achieved in two steps. Initially, we have the R-parity conserved interactions between the gravitino, one SM fermion and the corresponding scalar super-partner, which in principle do not allow the direct decay of the gravitino. If we represent the SM fermions by ψ , the scalar super-partners as ϕ and the gravitino field as Ψ_μ , we can write the Lagrangian associated to this interaction as:

$$\mathcal{L} = \frac{1}{\sqrt{2}M_*} \bar{\psi}_L \gamma^\mu \gamma^\nu \partial_\nu \phi \Psi_{\mu R} \quad (2.1)$$

where the L/R indices standing for left/right chirality, γ^μ being the Dirac matrices and $M_* = (8\pi GN)^{-1/2} = 2.4 \times 10^{18}$ GeV the reduced Planck mass. In this notation the mass of the gravitino is given by $m_G = F/\sqrt{3}M_*$, with F the scale of spontaneous-SUSY breaking.

In order to allow gravitino decays we consider trilinear RpV interactions between the scalar super-partners and pairs of SM fermions. This part contains the trilinear couplings that ultimately determine the channels allowed for gravitino decays. The superpotential that generate the RpV interactions can be written in terms of the left-handed superfields for the leptons (L), quarks (Q) and Higgs of hypercharge 1/2 (H) and the right-handed superfields for the charged leptons (E^c), up and down type quarks (U^c , D^c). In practice, this superpotential is given by the following expression,

$$W_{\mathcal{R}_p} = \sum_{ijk} \left(\frac{1}{2} \lambda_{ijk} L_i L_j E_k^c + \lambda'_{ijk} L_i Q_j D_k^c + \lambda''_{ijk} U_i D_j D_k^c + \epsilon_i H L_i \right) \quad (2.2)$$

where i, j, k are flavor indices, λ_{ijk} , λ'_{ijk} , λ''_{ijk} are dimensionless coupling constants and ϵ_i are dimension one parameters. Basically, for our analysis we just consider the first term of the superpotential, since we focus on the purely leptonic decay channels. In [19], we can find the analytical expressions for the decay rates for every combination of leptons in the final state, each one being proportional to just one λ_{ijk} constant.

In our analysis we classify the possible gravitino final state configurations by considering the cases that would produce in principle a different spectrum of electrons or positrons, those are given in Table (1). Because the final state is equivalent, each channel can contain any neutrino flavor. Therefore the relation between branching fractions and individual trilinear couplings is not necessarily direct.

Considering the effective channels given in Table (1), we can model the amount of electrons, positrons, or γ rays (labeled by η) produced on gravitino decays as:

$$\Phi_G^\eta(E) = \frac{1}{m_G \tau_G} \sum_{j=1}^9 Br_j \frac{dN_j^\eta}{dE} D_{\text{factor}}^\eta, \quad (2.3)$$

Channel	Final State
c1	$e^+\mu\nu$
c2	$e^+\tau\nu$
c3	$e^-\mu^+\nu$
c4	$\mu^-\mu^+\nu$
c5	$\tau^-\tau^+\nu$
c6	$\tau^-\mu^+\nu$
c7	$\tau^+\mu^-\nu$
c8	$e^-e^+\nu$
c9	$e^-\tau^+\nu$

Table 1. Independent channels considering prompt final states. Notice that we use ν to indicate any flavor of neutrinos.

with m_G and τ_G the mass and lifetime of the gravitino respectively. The term $\eta = e, p, \gamma$ for electron, positron or gamma-ray flux correspondingly. The D_{factor}^η is proportional to the density of dark matter in the case of $\eta = \gamma$, in the other cases is a more complex term that depends on the dark matter density and the propagation of charged particles in the Galaxy. The term dN_j^η/dE is the amount of electrons, positrons, or gamma-rays produced per energy and propagated at the Earth position and Br_j is the branching fraction of the corresponding channel.

2.1 Electron-positron spectrum

For the computation of the electron-positron spectrum at Earth's position, we consider an approach similar to that used in our previous work [18], therefore we suggest to follow that work and references therein, to check the details on the total flux computations, including propagation effects. For simplicity, we restrict the current analysis to the MED propagation working point only.

Now, let's focus on the spectrum of charged leptons. In principle, we can get each branching fraction as a function of the free parameters of our model, such as the trilinear couplings λ_{ijk} or the mass of scalars³. In general, however, we can consider the branching fractions as the effective free parameters for the fit of charged lepton measurements satisfying the condition $\sum_i Br_i = 1$.

Considering that some of the channels generate the same spectrum of electrons (positrons), we can reduce the model degrees of freedom further by grouping decay channels as follows⁴:

$$\Phi_G^e(E) \propto \frac{1}{m_G \tau_G} \left[\alpha_1 \frac{dN_1^e}{dE} + \alpha_2 \frac{dN_2^e}{dE} + \alpha_3 \frac{dN_3^e}{dE} \right] \quad (2.4)$$

where $\alpha_1 = Br_1 + Br_4 + Br_7$, $\alpha_2 = Br_2 + Br_5 + Br_6$ and $\alpha_3 = Br_3 + Br_8 + Br_9$ with $\alpha_1 + \alpha_2 + \alpha_3 = 1$. Thus, we just need to define two independent effective branching fractions for fitting the electron spectrum. Similarly, for the positron spectrum we have that⁵

³At some point we have to do this computation, for which we suggest to follow hep-ph/0107286

⁴I think we need to explain better why some of the spectrum we obtain are equal, this is not obvious, at least for me

⁵I'm not sure the following equation is right! could someone check?

$$\Phi_G^p(E) \propto \frac{1}{m_G \tau_G} \left[(Br_1 + Br_2 + Br_8) \frac{dN_1^p}{dE} + (Br_3 + Br_4 + Br_6) \frac{dN_3^p}{dE} + (Br_5 + Br_7 + Br_9) \frac{dN_3^p}{dE} \right]$$

Additionally, we can use the equivalence between branching fractions of conjugated decay channels, $Br_1 = Br_3$, $Br_2 = Br_9$ and $Br_6 = Br_7$, to rewrite the positron spectrum as:

$$\begin{aligned} \Phi_G^p(E) &\propto \frac{1}{m_G \tau_G} \left[(Br_9 + Br_3 + Br_8) \frac{dN_1^p}{dE} + (Br_1 + Br_4 + Br_7) \frac{dN_3^p}{dE} + (Br_2 + Br_5 + Br_6) \frac{dN_5^p}{dE} \right] \\ \Phi_G^p(E) &\propto \frac{1}{m_G \tau_G} \left[\alpha_1 \frac{dN_3^p}{dE} + \alpha_2 \frac{dN_5^p}{dE} + \alpha_3 \frac{dN_1^p}{dE} \right] \end{aligned}$$

Finally, we can use that the electron spectrum from a given channel must be equal to the positron spectrum of the conjugated one to find that

$$\Phi_G^p(E) \propto \frac{1}{m_G \tau_G} \left[\alpha_1 \frac{dN_1^e}{dE} + \alpha_2 \frac{dN_2^e}{dE} + \alpha_3 \frac{dN_3^e}{dE} \right] \quad (2.5)$$

$$\Phi_G^p(E) = \Phi_G^e(E) \quad (2.6)$$

Therefore, for the fit of AMS-02, CALET or DAMPE data we just need two alpha parameters and three independent spectra. Our model automatically produces electron-positron symmetry for (gravitino) dark matter decays, as expected from general arguments of charge conjugation symmetry.

2.2 Gamma-ray spectrum

Analogously to the electron-positron flux, we may discuss the total contribution of gravitino decays to the EGB measured at Earth's position by considering the following expression

$$\Phi_G^\gamma(E) \propto \frac{1}{m_G \tau_G} \sum_{i=1}^9 Br_i \frac{dN_i^\gamma}{dE} \quad (2.7)$$

In this case we are not going to exploit the potential similarities between the gamma-ray energy spectra arising from different decay channels, if they exist at all. Instead, we are going to use the results of the previous section to find scenarios where the gamma-ray spectrum is small enough to be compatible with the EGB measurements (or limits).

To match the photon spectrum, we still have additional freedom to choose the branching fractions. Because the fit to charged leptons merely constrain the branching ratio sums α_1 , α_2 and α_3 . Also we must notice that for the photon spectrum we do not have coincidences between the spectrum of different channels such as $e^+ \mu^- \nu$ and $e^+ \tau^- \nu$, as we had for positrons. Therefore, we are free to choose Br_1 to Br_9 subject to the following conditions:

$$\begin{aligned}
\alpha_1 &= Br_1 + Br_4 + Br_7 \\
\alpha_2 &= Br_2 + Br_5 + Br_6 \\
\alpha_3 &= Br_3 + Br_8 + Br_9
\end{aligned}$$

plus $Br_1 = Br_3$, $Br_2 = Br_9$ and $Br_6 = Br_7$. Thus, in order to lower the number of photons produced we choose Br_i in the following way,

$$\begin{aligned}
Br_4 &= \alpha_1, \quad Br_1 = Br_3 = 0 \\
Br_5 &= \alpha_2, \quad Br_2 = Br_9 = 0 \\
Br_8 &= \alpha_3, \quad Br_6 = Br_7 = 0
\end{aligned}$$

which can be justified from the analysis of the gamma-ray spectra obtained for the corresponding channels. Basically, we prioritize the channels that produce the least amount of photons per gravitino decay.⁶

3 Statistical data analysis

3.1 Dataset definition

Motivated by the anomalous positron fraction measured by PAMELA [3] and AMS-02 [4], in this work, we study a model of dark matter that try to accomodate old and recent data concerning the detection of electrons and positrons cosmic ray fluxes on earth position, which are originated in astrophysical environments. Also we use the measurements of gamma-rays from Fermi-LAT [9] in order to check the gamma ray component of our models. Specifically, we consider the following datasets:

- D_1 : The positron fraction measured by AMS-02 between 0.5 and 500 GeV [4],
- D_2 : The independent measurement of the electron and positron fluxes by AMS-02 between 0.5 and 700 GeV [5],
- D_3 : The measurement of the sum of electron and positron spectrum measured by AMS-02 between 0.5 GeV and 1 TeV [6],
- D_4 : The extended measurement of the sum of electron and positron spectrum by CALET between 11 GeV and 4.8 TeV [7],
- D_5 : The direct detection of the spectrum of electrons plus positrons measured by DAMPE between 25 GeV and 4.6 TeV [8] and
- D_6 : The spectrum of isotropic diffuse gamma-ray emission between 100 MeV and 820 GeV measured by Fermi-LAT [9], from which we derive the limits on the EGB,

where D_i identify each analysed dataset, those will be useful during the implementation and discussion of our statistical analysis in the rest of this section.

⁶Maybe, this choice needs further justification but in principle it has allowed us to find compatible points, which can be seen from the plots shown in the analysis part.

3.2 Fitting cosmic ray flux data

We fit measurements related to electron and positron fluxes at Earth's position. First, we define backgrounds for each of these fluxes with power laws:

$$\Phi_B^p(E) = C_p E^{-\gamma_p}, \quad (3.1)$$

for positrons, and for electrons:

$$\Phi_B^e(E) = C_e E^{-\gamma_e}. \quad (3.2)$$

It has been shown [?] ⁷ that is not possible to reproduce the rise in electron and positron flux above ≈ 200 GeV modeling the fluxes with decreasing power laws. Therefore, we must include a source term injecting electrons and positrons at high energies. Our source term comes from the decay of gravitino dark matter into standard model particles, whose general expression is given in Eq. (2.3). It is worth noticing that gravitino decay yields equal amounts of electrons and positrons, as shown in Eq. (2.6).

Considering the definition of our background model and the analysis of the gravitino sector of the previous section, we end up with eight free parameters that need to be fixed to fully determine signal and background for electron and positron fluxes. Therefore, in order to compare with data, for instance positron measurements $\Phi_D^p(E_i)$, we define the following Gaussian likelihood form:

$$\log \mathcal{L}_{\text{Positrons}} = -\frac{1}{2} \sum_i \left(\frac{(\Phi_D^p(E_i) - \Phi_M^p(\theta_p, E_i))^2}{(\sigma_D^2 + j \times (\Phi_D^p(\theta_p, E_i))^2)} - \frac{1}{(\sigma_D^2 + j \times (\Phi_D^p(\theta_p, E_i))^2)} \right), \quad (3.3)$$

with σ_D the statistical uncertainty of the measurement. The model is defined as:

$$\Phi_M^p(\theta, E) = \Phi_B^p(C_p, \gamma_p, E) + \Phi_G^p(m_G, \tau_G, \alpha_1, \alpha_2, E). \quad (3.4)$$

The parameter j increases the nominal uncertainty by a fraction of the model, to account for systematic effects and correlations among different data sets [8]. The likelihood functions considering other measurements can be defined analogously ⁹. In order to explore the full likelihood, find the best fit values and credible regions of our unknown parameters, we use the Bayesian inference package Multinest [20] through its Python interface PyMultinest [21]. We analyse our datasets in four different cases by considering sets of 3 or 4 measurements. These cases are given by:

- Case 1: $D_1 + D_2$
- Case 2: $D_1 + D_2 + D_3$
- Case 3: $D_1 + D_2 + D_4$
- Case 4: $D_1 + D_2 + D_5$

⁷Does this needs to e demonstrated?, this is not just obvious?

⁸ref to Hogg/emcee/? or someone else who does this?.

⁹app or reference to the jupyter-notebook

Parameter	Case 1	Case 2	Case 3	Case 4
C_p [1/GeV cm ² s str]	14.90	14.74	14.93	14.37
γ_p	3.11	3.10	3.11	3.09
C_e [1/GeV cm ² s str]	426.10	421.77	422.08	422.67
γ_e	3.27	3.27	3.27	3.27
m_G [GeV]	1281	2274	3604	3751
τ_G [10 ²⁶ s]	4.61	3.59	2.27	2.29
$\alpha_1 : \mu^- l^+ \nu$	0.03	0.36	0.15	0
$\alpha_2 : \tau^- l^+ \nu$	0.54	0.58	0.82	0.68
$\alpha_3 : e^- l^+ \nu$	0.43	0.06	0.03	0.32

Table 2. Best fit parameters for the different cases defined in previous section. Recall that $\alpha_3 = 1 - (\alpha_1 + \alpha_2)$ by definition.

In this way, we consider the majority of currently available charged leptons measurements. Additionally, we will study how each of them affect gravitino and background parameters. As a final target, for each model case, we predict the EGB¹⁰ and compare to Fermi-LAT measurements (D6).

4 Results

The results of our statistical analysis are summarized in table 2 and Figures 3 and 2 shown at the end of the section. In general we can see that the required life-time τ_G to fit the charged-lepton data is around 4×10^{26} s. We find that this value is sufficiently high to predict a gamma-ray flux statistically compatible with the limits of the EGB. Below, we present details of the results of our effective analysis for the different datasets considered.

4.1 $D_1 + D_2$

This is our baseline dataset, in this case, we only include the AMS-02 measurements of the electron and positron flux and the positron fraction. We found many solutions that can fit well the lepton data, while not overshooting the EGB. This is in contrast to the bilinear model in our previous work, which overpass the EGB constrain.

4.2 $D_1 + D_2 + D_3$

We get similar results as in the previous case, but adding the electron-positron sum measured by AMS-02 too.¹¹

4.3 $D_1 + D_2 + D_4$

In this case we do not use the electron-positron sum from AMS-02, but the values reported by CALET. The CALET spectrum is compatible with results from AMS-02, but not with Fermi and DAMPE data. Including CALET data makes the fit to prefer higher gravitino masses

¹⁰Do we really predict the EGB? I guess we don't...

¹¹Not entirely sure what it means, but the parameter related to this new measurement $\log(k)$ is significantly larger than the other three (see slide 8), maybe some correlation with the other data. An interpretation is that to produce the observed points we need to degrade the likelihood in the electron+positron data in a fraction of the model.

and reduce the parameter space allowed for reproducing the lepton data while keeping the gamma-ray flux below the Fermi estimation.

4.4 $D_1 + D_2 + D_5$

We include here the electron-positron sum from DAMPE. This measurement is in tension with AMS02. We find no points compatible with lepton and gamma-ray data¹².

5 Comparison between trilinear and bilinear cases

We now compare the bi-linear to tri-linear decay channel modes, i.e., our previous and current work. In the BRpV case only two-body decays containing gauge bosons and leptons ($G \rightarrow Z\nu$ and $G \rightarrow W^\pm l^\mp$) or a Higgs particle plus neutrinos ($G \rightarrow H\nu$) are considered. In particular, in our previous work we have shown that the preferred channel to fit the positron anomaly is given by $G \rightarrow W^\pm \tau^\mp$, which is one of the channels that produce more final state photons, instead, in TRpV we only model three-body decays including two charged leptons plus a neutrino ($G \rightarrow l^\pm l^\mp \nu$) as shown in table 1. In the previous section we have shown that the preferred channels are given by $G \rightarrow \tau^\pm l^\mp \nu$, with l^\mp including the three flavours, but also the contributions of other channels are necessary.

Interestingly, from the analysis of the propagated spectrum of charged leptons associated to these channels, which are shown in Fig. (1), we see that TRpV produces more charged leptons than BRpV. In order to support this argument we have computed the total spectrum of charged leptons for both cases considering branching fractions that fit well the positron anomaly, but considering a normalized and common life-time. In simple words, in TRpV we need a lower rate of gravitino decays in comparison to BRpV to fit the positron anomaly.

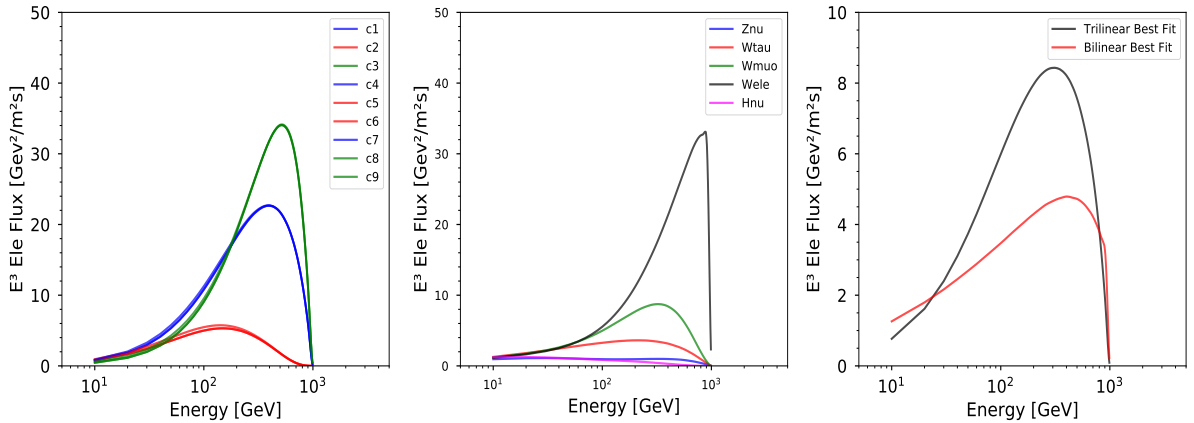


Figure 1. Charged lepton spectrum of trilinear and bilinear decay modes are shown at the left and center pictures respectively, the best fit for both cases are shown on the right picture.

Furthermore, it can also be shown by an analogous exercise using the photon spectrum, shown in Fig. (2), that the contribution from TRpV is smaller to the one obtained in the BRpV case. Therefore, there are two contributing factors improving the performance of TRpV in comparison to BRpV. For a given gravitino decay rate, there are both an enhancement

¹²Sentence not clear, need to rewrite

of the charged lepton flux and a reduction of the contribution to photons that conspire to reduce the tension with the EGB measurements.

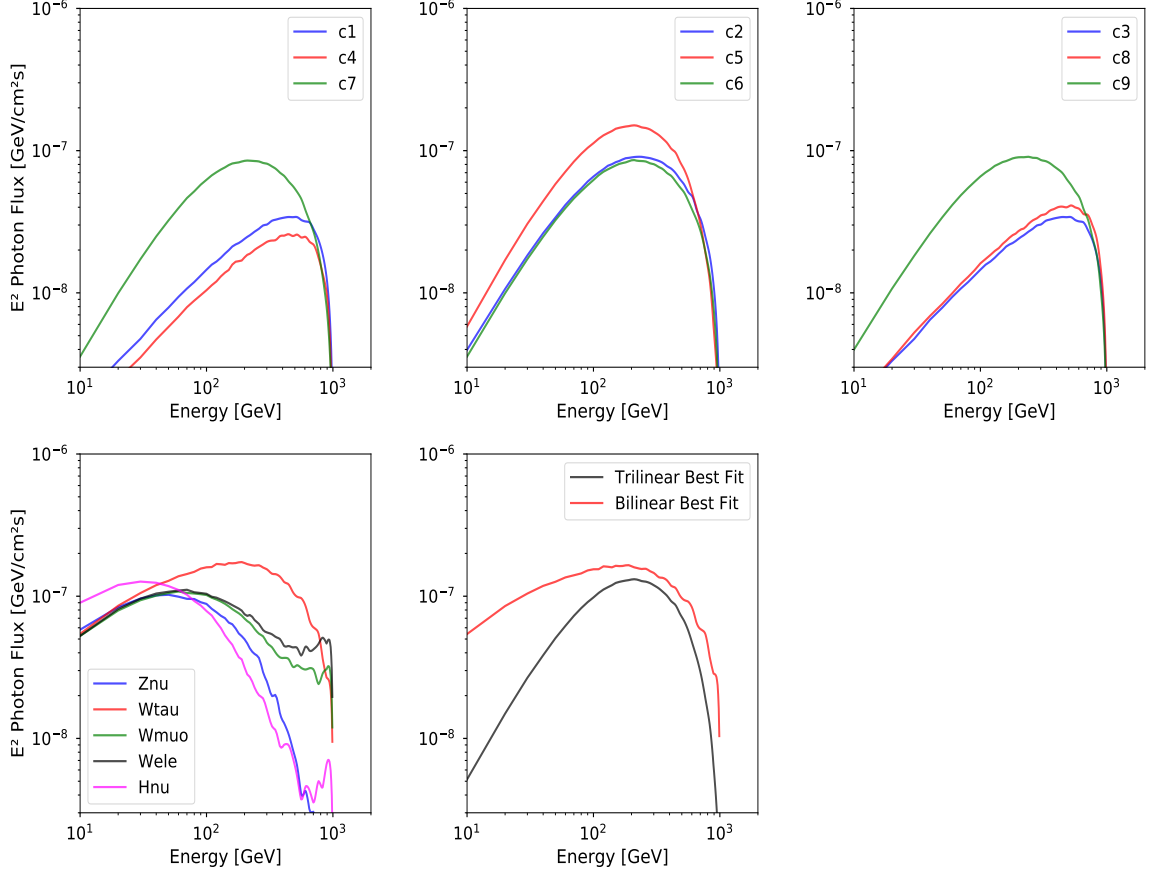


Figure 2. Photon spectrum of trilinear (full top row) and bilinear (left bottom panel) decay channels. In the last figure (right bottom panel) we show the contribution to photons from both cases considering branching fractions that fit well the positron spectrum.

6 Conclusions

We have presented a tri-linear gravitino decay model. Within this scenario, we can consistently model AMS-02 data while respecting the EGB limit derived from Fermi-LAT data, which can be understood from the particular features of gravitino decays of this model¹³. However, when we include the data from CALET or DAMPE, that cover higher energies than AMS-02, tensions appear in the interpretation of the data from the different experiments. Last but not least, in this model we can also connect the life-time and branching fractions of gravitino decays obtained by fitting the positron anomaly to the scale of neutrino physics.

In our computations we have not considered the extragalactic component of gravitino decays or the inverse Compton mechanism, which will enhance the contribution to the total

¹³Need to rephrase this sentence certainly

amount of gamma-rays produced by our candidate dark matter. By considering these issues we may suggest that this scenario can accomodate most but not all of the anomalous signal in the charged lepton measurements and the rest should be supplied by astrophysical components.¹⁴

Acknowledgments

We acknowledge support from the CONICYT-Chile grants Basal-CATA PFB-06/2007 and Basal AFB-170002 (JB), FONDECYT Postdoctorados 3160439 (JB) and the Ministry of Economy, Development, and Tourism's Millennium Science Initiative through grant IC120009, awarded to The Millennium Institute of Astrophysics, MAS (JB). BP also thanks for the support of the State of São Paulo Research Foundation (FAPESP). E.C. is supported by chilean grants; FONDECYT No. 11140549 and No. 1190886, and in part by CONICYT Basal FB0821 grant.

A Appendix

A.1 Results of the fit

In this section we show the plots concerning the statistical analysis of Cases 1 to 4, which are detailed in the main text. The black lines indicate the best fit curve, while the shade regions show 1 and 2 σ confidence level regions¹⁵.

B Appendix: Discussion about the gravitino lifetime and neutrino masses

The full expressions for the gravitino decay width, considering trilinear R-Parity violation, are given in [19]. For instance, from these expressions we can get an approximated formula for the leptonic decay $\Gamma(\tilde{G} \rightarrow \nu_i e_j \bar{e}_k)$ by assuming that the mass of the sleptons mediating the three body decay are equal, such that $m_{\tilde{\nu}_{iL}} = m_{\tilde{e}_{jL}} = m_{\tilde{e}_{kR}} = \tilde{m}$, and expand in taylor series around the variable m_G/\tilde{m} to obtain

$$\Gamma(\tilde{G} \rightarrow \nu_i e_j \bar{e}_k) \approx \frac{1}{96(2\pi)^3} \frac{\lambda_{ijk}^2}{8M_\star^2} \frac{m_G^7}{\tilde{m}^4}, \quad (\text{B.1})$$

This result shows that the decay width (lifetime) decreases (increases) rapidly as we increase \tilde{m} , as expected. We expect that a similar behavior should be obtained even when the mass of sleptons are not equal.

Indeed, we have verified this expectation numerically, by evaluating the full expression given in [19] using the maximum numerical precision in Mathematica. For instance, in Fig. 8 we plot the gravitino lifetime as a function of $m_{\tilde{\nu}_{iL}}$ for $m_{\tilde{e}_{jL}} = m_{\tilde{\nu}_{iL}}/2$ and $m_{\tilde{e}_{kR}} = m_{\tilde{\nu}_{iL}}/5$. Also, in the same figure we plot the lifetime derived from Eq. B.1 evaluated at $\tilde{m} = m_{\tilde{\nu}_{iL}}/2$ in order to check that both approaches, exact computation and approximated formula, behave similarly.

Therefore, we can confidently derive the following expression for the gravitino lifetime,

¹⁴Can we said something about the order of those effects? if they are small or very small we can said for instance that in the first approximation we are fine, and that we could include these effects in a future publication?

¹⁵I think we may move some of these plots to the main body of the paper, we can discuss about which of them are more important.

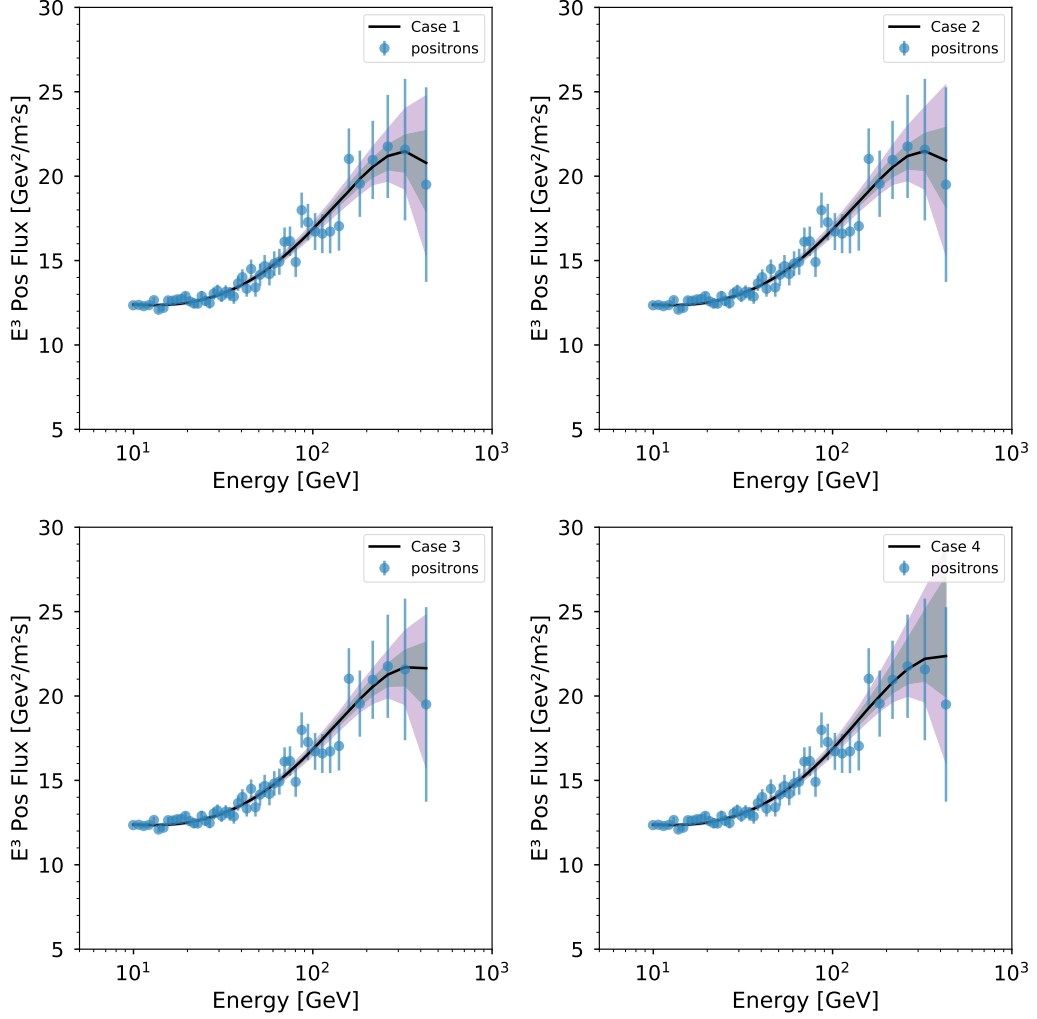


Figure 3. Best fit results for positron flux. The cases D_1 to D_4 are ordered from left to right and from top to bottom.

$$\tau_G \approx 10^{26} \text{ s} \left(\frac{1}{\lambda_{ijk} \lambda_{ijk}} \right) \left(\frac{\tilde{m}}{2 \times 10^7 \text{ GeV}} \right)^4 \left(\frac{1 \text{ TeV}}{m_G} \right)^7 \quad (\text{B.2})$$

where we have normalized with respect to 10^{26} s since this is the order of magnitude required by experiments such as AMS-02 and Fermi-LAT in order to fit the electron positron data in the first case or to avoid gamma ray constraints in the second.

In TRpV the neutrino mass matrix receives contributions from 1-loop diagrams that contain both a charged lepton and the corresponding slepton. Indeed, we have derived the following (preliminary) expression¹⁶

¹⁶Why preliminary?

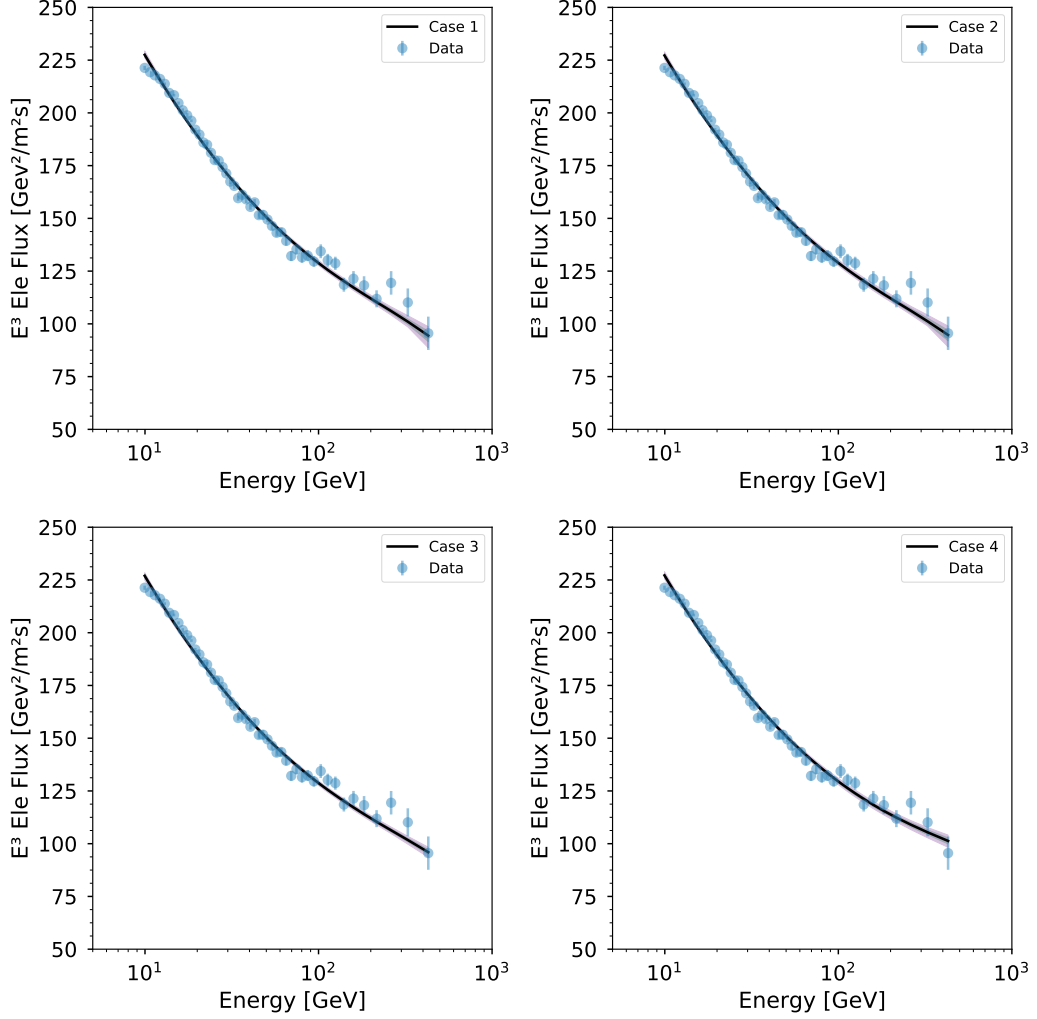


Figure 4. Best fit results for electron flux. The cases D_1 to D_4 are ordered from left to right and from top to bottom.

$$M_{ij}^{\nu(1)} \approx \frac{1}{16\pi^2} \sum_{gr} s_{\tilde{l}} c_{\tilde{l}} (\lambda_{igr} \lambda_{jrg} + \lambda_{jgr} \lambda_{irg}) m_g \ln \frac{m_{\tilde{l}_{r2}}^2}{m_{\tilde{l}_{r1}}^2}$$

where i and j are neutrino generation indices that runs from 1 to 3. g is a charged lepton index that also run from 1 to 3, as well as r which is a slepton index. Thus, it can be seen that for order one parameters, $s_{\tilde{l}} \sim c_{\tilde{l}} \sim \ln(m_{\tilde{l}_{r2}}^2/m_{\tilde{l}_{r1}}^2) \sim 1$, we can get neutrino masses around the eV scale for $\lambda_{ijk} \approx 0.01$ even for $m_g \approx m_e$.

Indeed, by following the expressions given in [22] for the contribution of λ' trilinear terms, we can get by analogy that the dominant term in the leptonic sector is

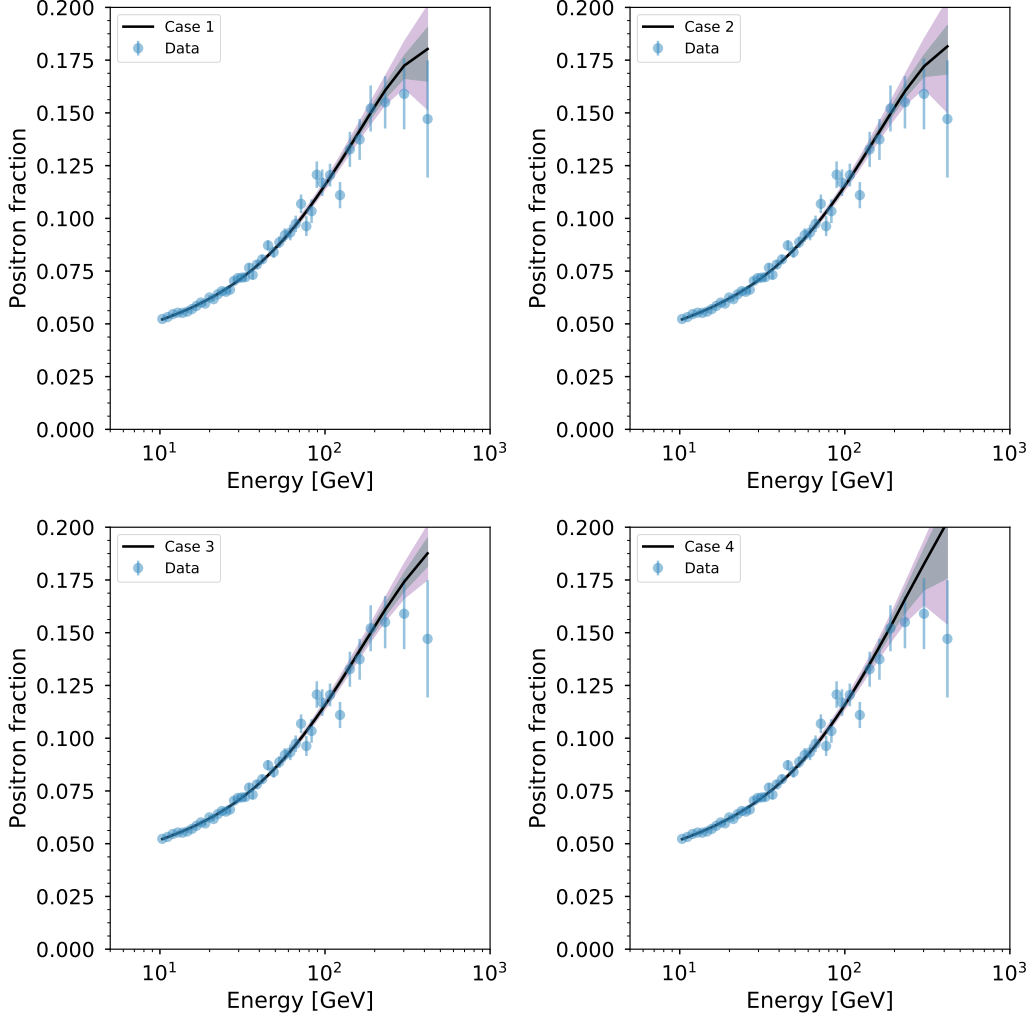


Figure 5. Best fit results for positron fraction. The cases D_1 to D_4 are ordered from left to right and from top to bottom.

$$\begin{aligned}
M_{ij}^{\nu(1)} &\approx \frac{1}{8\pi^2} \lambda_{i23} \lambda_{j32} \frac{m_\mu m_\tau A_\tau}{\tilde{m}^2} \\
&\approx 2 \times 10^{-2} \text{eV} \lambda_{i23} \lambda_{j32} \left(\frac{10^8 \text{ GeV}}{\tilde{m}} \right) \\
&\approx 2 \times 10^{-2} \text{eV} (\lambda_{i23} \lambda_{j32})^{1/4} \left(\frac{\tau_G}{10^{26} \text{ s}} \right)^{1/4} \left(\frac{m_G}{2 \text{ TeV}} \right)^{7/4}
\end{aligned}$$

where A_τ is a free parameter that can be considered of order \tilde{m} , as it is done in [22]. Thus, if we consider this formula together with Eq. (B.2) we see that we can have contributions to the neutrino mass matrix of order 10^{-2} eV for trilinear couplings and a scalar mass¹⁷ which are compatible with $\tau_G \approx 10^{26}$ s.

¹⁷...and a scalar mass of what order, it seems that the end of the sentence is missing here

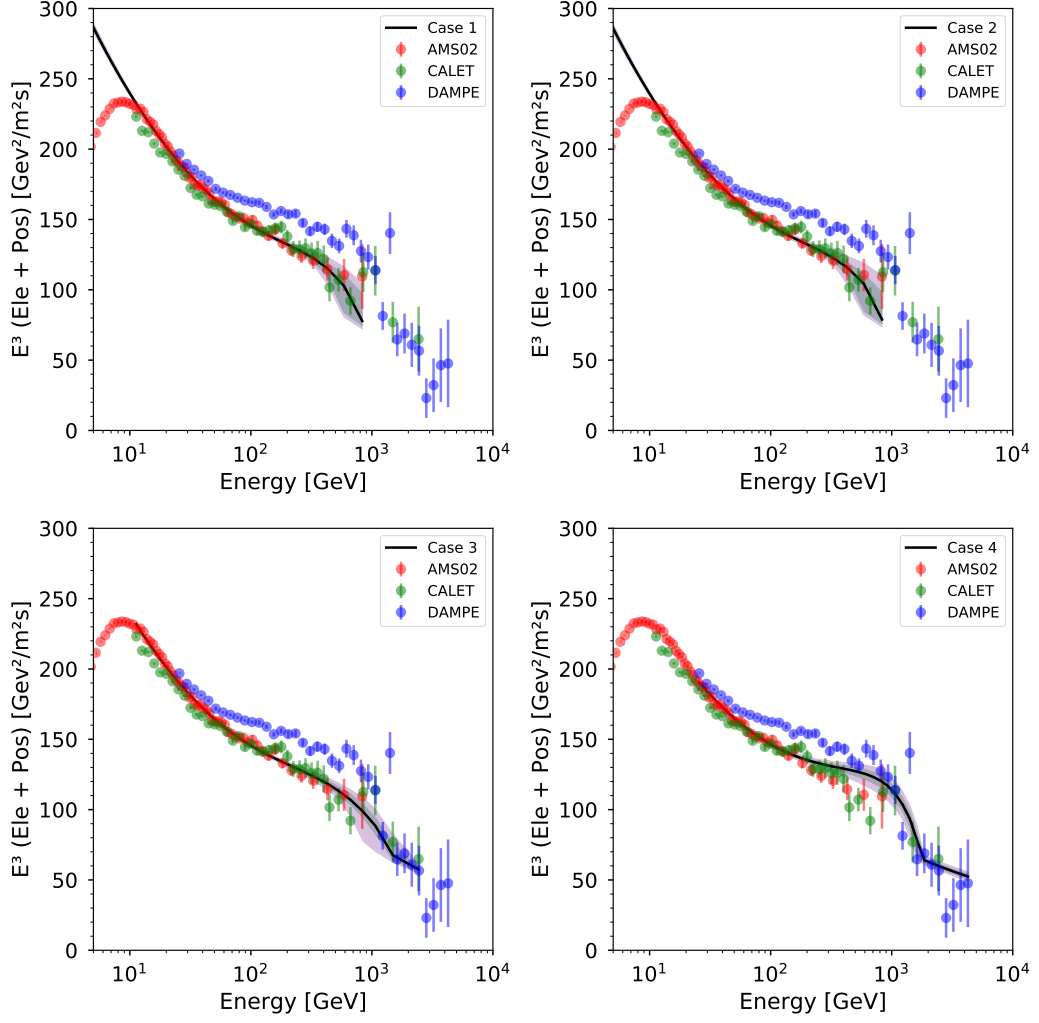


Figure 6. Best fit results for electron plu positron flux. The cases D_1 to D_4 are ordered from left to right and from top to bottom.

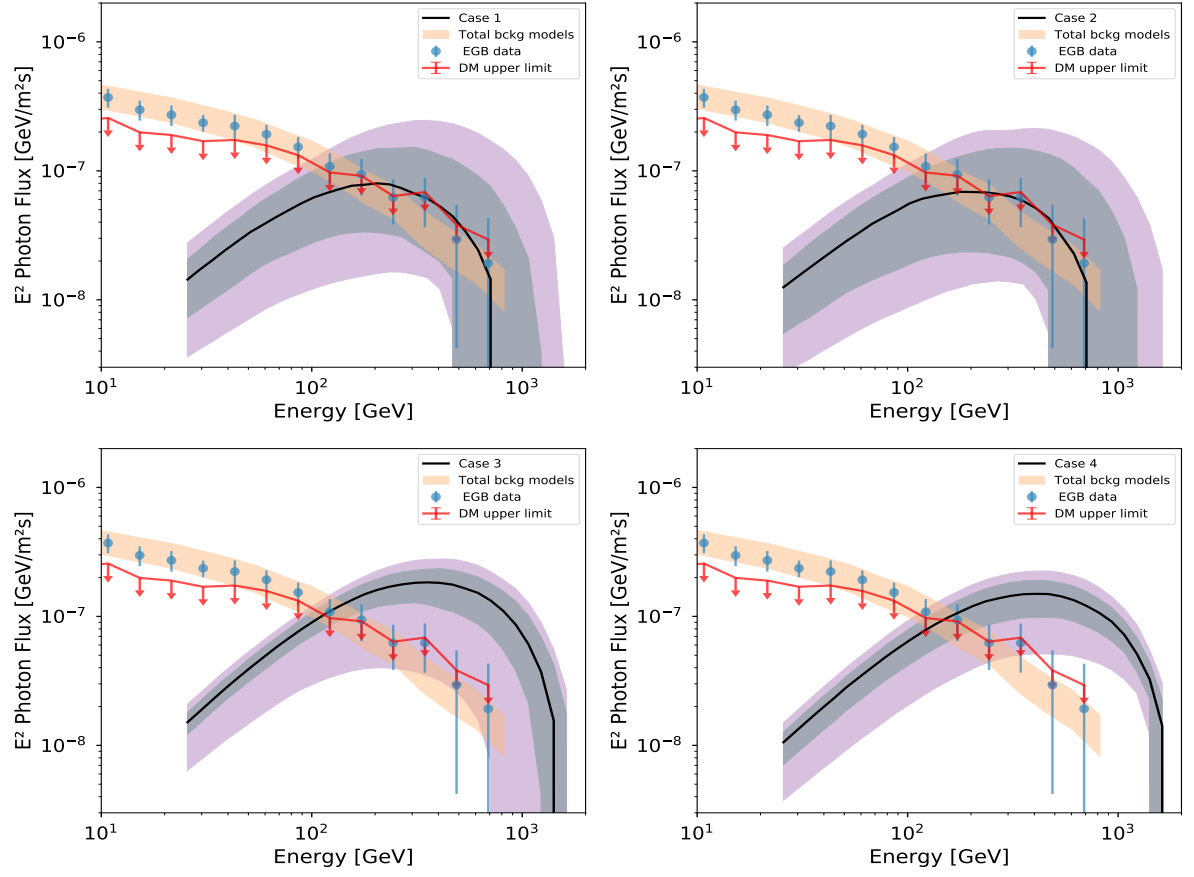


Figure 7. Best fit results for photon flux compared to EGB limits. The cases D_1 to D_4 are ordered from left to right and from top to bottom.

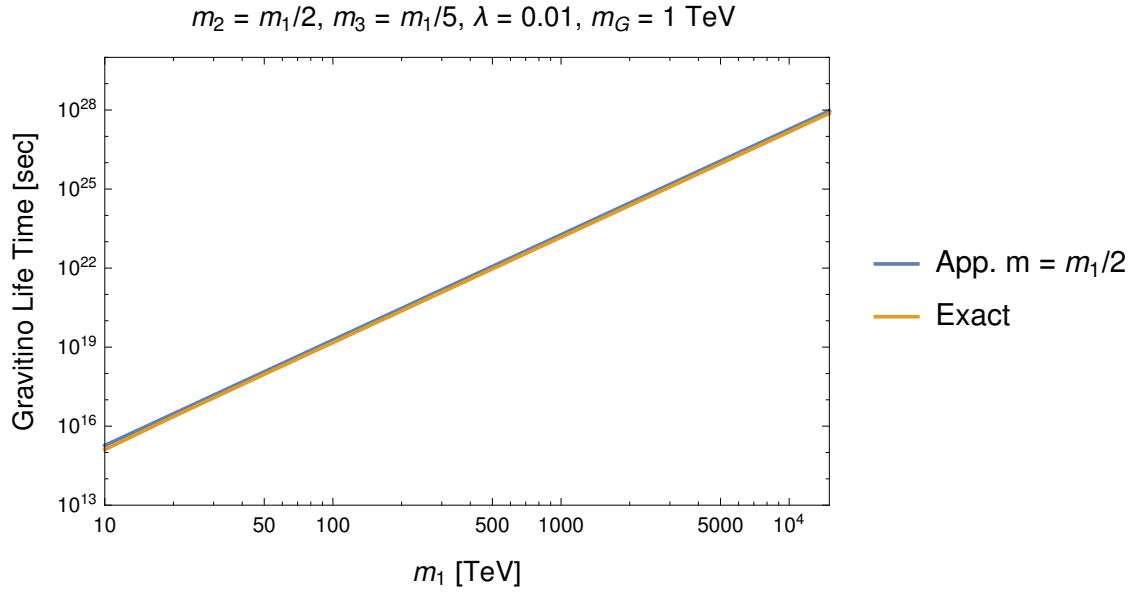


Figure 8. Gravitino life time in Trilinear RpV for $\lambda_{ijk} = 0.01$, $m_G = 1 \text{ TeV}$. For simplicity we use m_1, m_2, m_3 and m instead of $m_{\tilde{\nu}_{iL}}, m_{\tilde{e}_{jL}}, m_{\tilde{e}_{kR}}$ and \tilde{m} .

References

- [1] M. Grefe, *Unstable Gravitino Dark Matter - Prospects for Indirect and Direct Detection*, [arXiv:1111.6779](#).
- [2] D. Hooper, *TASI Lectures on Indirect Searches For Dark Matter*, [arXiv:1812.0202](#).
- [3] **PAMELA** Collaboration, O. Adriani et al., *An anomalous positron abundance in cosmic rays with energies 1.5-100 GeV*, *Nature* **458** (2009) 607–609, [[arXiv:0810.4995](#)].
- [4] **AMS** Collaboration, L. Accardo et al., *High Statistics Measurement of the Positron Fraction in Primary Cosmic Rays of 0.5500 GeV with the Alpha Magnetic Spectrometer on the International Space Station*, *Phys. Rev. Lett.* **113** (2014) 121101.
- [5] **AMS** Collaboration, M. Aguilar et al., *Electron and Positron Fluxes in Primary Cosmic Rays Measured with the Alpha Magnetic Spectrometer on the International Space Station*, *Phys. Rev. Lett.* **113** (2014) 121102.
- [6] **AMS** Collaboration, M. Aguilar et al., *Precision Measurement of the $(e^+ + e^-)$ Flux in Primary Cosmic Rays from 0.5 GeV to 1 TeV with the Alpha Magnetic Spectrometer on the International Space Station*, *Phys. Rev. Lett.* **113** (2014) 221102.
- [7] O. Adriani et al., *Extended Measurement of the Cosmic-Ray Electron and Positron Spectrum from 11 GeV to 4.8 TeV with the Calorimetric Electron Telescope on the International Space Station*, *Phys. Rev. Lett.* **120** (2018), no. 26 261102, [[arXiv:1806.0972](#)].
- [8] **DAMPE** Collaboration, G. Ambrosi et al., *Direct detection of a break in the teraelectronvolt cosmic-ray spectrum of electrons and positrons*, *Nature* **552** (2017) 63–66, [[arXiv:1711.1098](#)].
- [9] **Fermi-LAT** Collaboration, M. Ackermann et al., *The spectrum of isotropic diffuse gamma-ray emission between 100 MeV and 820 GeV*, *Astrophys. J.* **799** (2015) 86, [[arXiv:1410.3696](#)].
- [10] M. Grefe, *Neutrino signals from gravitino dark matter with broken R-parity*, [arXiv:1111.6041](#).
- [11] M. Cirelli, E. Moulin, P. Panci, P. D. Serpico, and A. Viana, *Gamma ray constraints on decaying dark matter*, *Phys. Rev. D* **86** (Oct., 2012) 083506, [[arXiv:1205.5283](#)].
- [12] S. Ando and K. Ishiwata, *Constraints on decaying dark matter from the extragalactic gamma-ray background*, *JCAP* **1505** (2015), no. 05 024, [[arXiv:1502.0200](#)].
- [13] M. Laletin, *A no-go theorem for the dark matter interpretation of the positron anomaly*, *Frascati Phys. Ser.* **63** (2016) 7–12, [[arXiv:1607.0204](#)].
- [14] W. Liu, X.-J. Bi, S.-J. Lin, and P.-F. Yin, *Constraints on dark matter annihilation and decay from the isotropic gamma-ray background*, *Chin. Phys. C* **41** (2017), no. 4 045104, [[arXiv:1602.0101](#)].
- [15] K. Belotsky, R. Budaev, A. Kirillov, and M. Laletin, *Fermi-LAT kills dark matter interpretations of AMS-02 data. Or not?*, *JCAP* **1701** (2017), no. 01 021, [[arXiv:1606.0127](#)].
- [16] S. Profumo, J. Reynoso-Cordova, N. Kaaz, and M. Silverman, *Lessons from HAWC pulsar wind nebulae observations: The diffusion constant is not a constant; pulsars remain the likeliest sources of the anomalous positron fraction; cosmic rays are trapped for long periods of time in pockets of inefficient diffusion*, *Phys. Rev.* **D97** (2018), no. 12 123008, [[arXiv:1803.0973](#)].
- [17] D. Hooper, I. Cholis, T. Linden, and K. Fang, *HAWC Observations Strongly Favor Pulsar Interpretations of the Cosmic-Ray Positron Excess*, *Phys. Rev.* **D96** (2017), no. 10 103013, [[arXiv:1702.0843](#)].
- [18] E. Carquin, M. A. Diaz, G. A. Gomez-Vargas, B. Panes, and N. Viaux, *Confronting recent AMS-02 positron fraction and Fermi-LAT extragalactic γ -ray background measurements with gravitino dark matter*, *Phys. Dark Univ.* **11** (2016) 1–10, [[arXiv:1501.0593](#)].

- [19] G. Moreau and M. Chemtob, *R-parity violation and the cosmological gravitino problem*, *Phys.Rev.* **D65** (2002) 024033, [[hep-ph/0107286](#)].
- [20] F. Feroz, M. P. Hobson, and M. Bridges, *MultiNest: an efficient and robust Bayesian inference tool for cosmology and particle physics*, *Mon. Not. Roy. Astron. Soc.* **398** (2009) 1601–1614, [[arXiv:0809.3437](#)].
- [21] J. Buchner, A. Georgakakis, K. Nandra, L. Hsu, C. Rangel, M. Brightman, A. Merloni, M. Salvato, J. Donley, and D. Kocevski, *X-ray spectral modelling of the AGN obscuring region in the CDFS: Bayesian model selection and catalogue*, *Astron. Astrophys.* **564** (2014) A125, [[arXiv:1402.0004](#)].
- [22] E. J. Chun and S. C. Park, *Neutrino mass from R-parity violation in split supersymmetry*, *JHEP* **01** (2005) 009, [[hep-ph/0410242](#)].